sign steady chaotic flows for use in microfluidic systems. A mixer based on patterns of grooves on the floor of the channel is shown schematically in Fig. 2A; we refer to this design as the staggered herringbone mixer (SHM). One way to produce a chaotic flow is to subject volumes of fluid to a repeated sequence of rotational and extensional local flows (*21*). This sequence of local flows is achieved in the SHM by varying the shape of the grooves as a function of axial position in the channel: The change in the orientation of the herringbones between half cycles exchanges the positions of the centers of rotation (local rotational flow, "c" in the Fig. 2A) and the up- and down-wellings (local extensional flow, "u" and "d" in Fig. 2A) in the transverse flow. Figure 2B shows the evolution of two streams through one cycle of the SHM.

In the SHM, the efficiency of mixing is controlled by two parameters: p, a measure of the asymmetry of the herringbones; and $\Delta\phi_m$, a measure of the amplitude of the rotation of the fluid in each half cycle (*22*). The angular displacement, $\Delta\phi_m$, is controlled by the geometry of the ridges (*20*) and the number of herringbones per half cycle (10 in the case shown in Fig. 2). As p goes to one-half (i.e., symmetric herringbones) or $\Delta\phi_m$ goes to zero, the flow becomes nonchaotic. For $p = 2/3$ and $\Delta\phi_m > 60°$, most of the cross-sectional area is involved in the chaotic flow (*23*). As in the twisting flow (Fig. 1), the form of flow in the SHM is independent of *Re* in the Stokes regime, and we have verified experimentally that it remains qualitatively the same for $Re < 100$.

The diagrams in Fig. 3, A to C, show the experiments we used to characterize mixing. At the entrance of the channel, distinct streams of a fluorescent and a clear solution fill opposite halves of the cross section of the channel. The micrographs in Fig. 3, A and B, show that for flows with high Péclet number ($Pe = 2 \times 10^5$), there is negligible mixing in a simple channel (Fig. 3A) and incomplete mixing in a channel with straight ridges (Fig. 3B) after the flow has proceeded 3 cm—the typical dimension of a microfluidic chip—down the channel. The confocal cross sections in Fig. 3C show that thorough mixing occurs at even higher Pe (9×10^5) in a channel that contains the SHM (*24*). The micrographs in Fig. 3C also show the rapid increase in the number of filaments and decrease in their thickness, Δr, as a function of the number of mixing cycles.

To quantify the degree of mixing (convection plus diffusion) as a function of the axial distance traveled in the mixer and of *Pe*, we measure the standard deviation of the intensity distribution in confocal images of the cross section of the flow like those in Fig. 3, A to C: $\sigma = \langle (I - \langle I \rangle)^2 \rangle^{1/2}$, where I is the grayscale value (between 0 and 1) of a pixel, and $\langle\ \rangle$ means an average over all the pixels in the image. The value of σ is

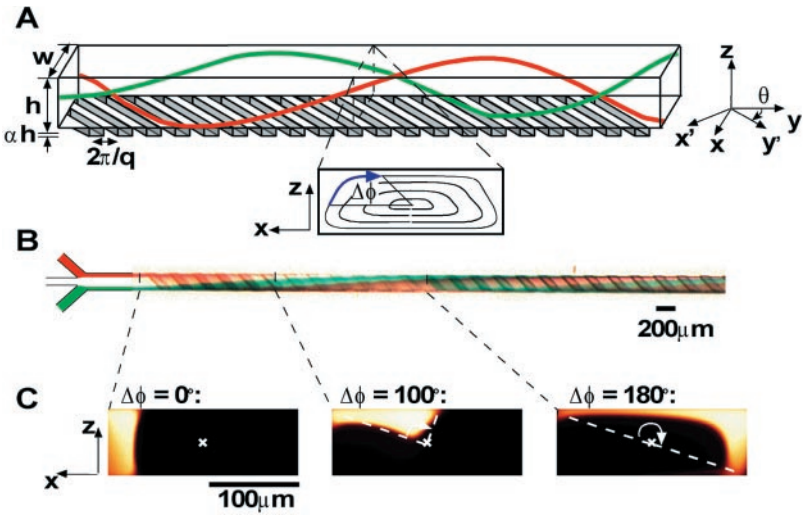

Fig. 1. Three-dimensional twisting flow in a channel with obliquely oriented ridges on one wall. (**A**) Schematic diagram of channel with ridges. The coordinate systems (x, y, z) and (x', y', z) define the principal axes of the channel and of the ridges. The angle θ defines the orientation of the ridges with respect to the channel. The amplitude of the ridges, αh, is small compared to the average height of the channel, h ($\alpha < 0.3$). The width of the channel is w and principal wavevector of the ridges is q. The red and green lines represent trajectories in the flow. The streamlines of the flow in the cross section are shown below the channel. The angular displacement, $\Delta\phi$, is evaluated on an outer streamline. (**B**) Optical micrograph showing a top view of a red stream and a green stream flowing on either side of a clear stream in a channel such as in (A) with $h = 70$ μm, $w = 200$ μm, $\alpha = 0.2$, $q = 2\pi/200$ μm^{-1}, and $\theta = 45°$. (**C**) Fluorescent confocal micrographs of vertical cross sections of a microchannel such as in (A). The frames show the rotation and distortion of a stream of fluorescent solution that was injected along one side of the channel such as the stream of green solution in (B). The measured values of $\Delta\phi$ are indicated (*29*).

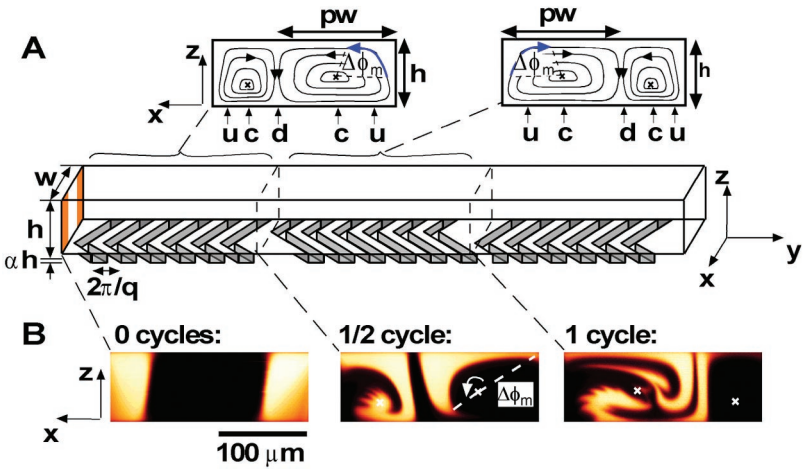

Fig. 2. Staggered herringbone mixer (SHM). (**A**) Schematic diagram of one-and-a-half cycles of the SHM. A mixing cycle is composed of two sequential regions of ridges; the direction of asymmetry of the herringbones switches with respect to the centerline of the channel from one region to the next. The streamlines of the flow in the cross section are shown schematically above the channel. The angle, $\Delta\phi_m$, is the average angular displacement of a volume of fluid along an outer streamline over one half cycle in the flow generated by the wide arms of the herringbones. The fraction of the width of the channel occupied by the wide arms of the herringbones is p. The horizontal positions of the centers of rotation, the upwellings, and the downwellings of the cellular flows are indicated by c, u, and d, respectively. (**B**) Confocal micrographs of vertical cross sections of a channel as in (A). Two streams of fluorescent solution were injected on either side of a stream of clear solution (*29*). The frames show the distribution of fluorescence upstream of the features, after one half cycle, and after one full cycle. The fingerlike structures at the end of the fluorescent filaments on the bottom left of the second two frames are due to the weak separation of streamlines that occurs in the rectangular grooves even at low *Re*. In this experiment, $h = 77$ μm, $w = 200$ μm, $\alpha = 0.23$, $q = 2\pi/100$ μm^{-1}, $p = 2/3$, and $\theta = 45°$, and there were 10 ridges per half cycle. $Re < 10^{-2}$. $\Delta\phi_m \sim 180°$.